Hofmeister Salts and Potential Therapeutic Compounds Accelerate in Vitro Fibril Formation of the N-Terminal Domain of PABPN1 Containing a Disease-Causing Alanine Extension†

Grit Lodderstedt,‡ Rolf Sachs,‡ Jürgen Faust,‡ Frank Bordusa,‡ Uwe Kühn,‡ Ralph Golbik,‡ Andreas Kerth,§ Elmar Wahle,‡ Jochen Balbach,|| and Elisabeth Schwarz*,‡

Institute for Biochemistry and Biotechnology of the Martin-Luther-University Halle-Wittenberg, Kurt-Mothes-Strasse 3, 06120 Halle, Germany, Institute of Physical Chemistry of the Martin-Luther-University Halle-Wittenberg, Mühlpforte 1, 06108 Halle, Germany, and Institute of Physics, Biophysics Group and "Mitteldeutsches Zentrum für Struktur und Dynamik der Proteine, MZP" of the Martin-Luther-University Halle-Wittenberg, Hoher Weg 8, 06120 Halle, Germany

Received July 5, 2007; Revised Manuscript Received October 24, 2007

ABSTRACT: The analysis of modulation of fibril formation helps to understand the mechanism of fibrillation processes besides opening routes for therapeutic intervention. Fibril formation was investigated with the N-terminal domain of the nuclear poly-A binding protein PABPN1, a protein in which mutation-based alanine extensions lead to the disease oculopharyngeal muscular dystrophy (OPMD). The disease is characterized by fibrillar inclusions consisting mainly of PABPN1. A systematic modulation of fibril formation kinetics was studied with trifluoroethanol, inorganic salts, low molecular weight organic substances, a poly-alanine peptide and anti-amyloidogenic compounds. Anions with salting out properties at high molar concentrations, poly-ethylene glycol and the poly-alanine peptide enhanced fibril formation rates. The effect of L-arginine on fibrillation rates depended on the counterion. Doxycycline and trehalose, compounds that have been found to mitigate OPMD symptoms in animal models, surprisingly accelerated fibril formation. Our results suggest that in the case of salts, primarily the salting out effects rather than electrostatic effects modulate fibril formation. The unexpected acceleration of fibril formation by trehalose and doxycycline questions the general view that these compounds per se impair fibril formation.

The nuclear poly(A) binding protein, PABPN1,[1] plays an important role in the length control of poly(A) tails (*1*, *2*). Trinucleotide extensions in the corresponding gene result in an extension of the wild type sequence of ten alanines positioned directly after the start methionine. In the most extreme case observed in humans, these extensions comprise seven additional alanines (*3*). The mutations have been shown to lead to the disease oculopharyngeal muscular dystrophy (OPMD). Afflicted individuals develop around the fifth decade typical OPMD-related symptoms like eyelid drooping, swallowing difficulties and proximal limb weakness. Histochemical analysis of biopsy material revealed intranuclear inclusions consisting primarily of PABPN1 (*4*−*8*). Costaining with antibodies and in situ hybridization with oligo(U) probes showed that the inclusions also contain ubiquitin, proteasomal subunits and poly(A) RNA (*6*). The inclusions were described as palisade-like deposits resembling amyloid fibrils with a diameter of ca. 8 nm.

Presently, numerous approaches are undertaken to clarify the disease causing molecular processes. Indirect evidence that OPMD may be caused by intranuclear protein deposits comes from mutant analysis demonstrating that oligomerization of PABPN1 facilitates protein aggregation (*9*). High local concentrations due to oligomerization are likely to support aggregation. Critical levels of PABPN1 alone may be sufficient for pathological conditions as already overexpression of wild type PABPN1 in a *Drosophila melanogaster* model elicited toxicity (*10*). Fine-tuning of PABPN levels by proteolytic breakdown is likely to play a role in disease development since the proteasome inhibitor lactacystin has been shown to act as an enhancer of PAPBN1 deposition and toxicity (*11*). On the other hand, critical levels of PABPN1 as the cause for OPMD do not stand in contrast to the hypothesis that the fibrils are the major cause for pathology because impaired proteolysis is supposed to increase critical threshold levels of PABPN1 that may be required for fibril formation. An involvement of PABPN1 deposits in disease development is supported by studies that demonstrate reduction of PABPN1 toxicity by chaperone

† This work was supported by the DFG through the Sonderforschungsbereich SFB 610.

* Corresponding author. E-mail: Elisabeth.Schwarz@biochemtech.uni-halle.de. Phone: + 49 345 55 24 856. Fax: + 49 345 55 27 013.

‡ Institute for Biochemistry and Biotechnology.

§ Institute of Physical Chemistry.

|| Institute of Physics, Biophysics Group and "Mitteldeutsches Zentrum für Struktur und Dynamik der Proteine, MZP".

[1] Abbreviations: ANS, 8-anilino-1-naphthalensulfonic acid; BOC, tert-butoxycarbonyl; CD, circular dichroism; EM, electron microscopy; Fmoc, (9*H*-fluoren-9-ylmethoxy) carbonyl; HBTU, 2-(1*H*-benzotriazole-1-yl)-1,1,3,3-tetramethylaelemmonium hexafluorophosphate; HOBt, 1-hydroxybenzotriazole; MALDI, matrix assisted laser desorption ionisation; NMP, 1-methyl-4-piperidone; NMR, nuclear magnetic resonance; OPMD, oculopharyngeal muscular dystrophy; PABPN1, nuclear poly(A) binding protein 1; PEG, poly-ethylene glycol; RP-HPLC, reversed phase high performance liquid chromatography; TFA, trifluoroacetic acid; TFE, trifluoroethanol.

10.1021/bi701322g CCC: $40.75 © 2008 American Chemical Society
Published on Web 01/19/2008

overexpression (*12*−*14*). Furthermore, certain low molecular weight compounds like doxycycline and trehalose attenuate OPMD-like symptoms in mouse models (*13*, *15*, *16*). It is, however, so far unclear whether these substances directly interact with fibrillar or prefibrillar protein species.

While the effects of low molecular weight substances on fibril formation can be tested in vivo, the influence of salts on fibrillation can only be tested in vitro. Salt-induced altered fibril formation rates have been demonstrated for insulin, β_2-microglobulin, α-synuclein, S6 and glucagon (*17*−*21*). In this work we present results that show that fibril formation kinetics can be modulated by salts, L-arginine, poly-ethylene glycol, a synthetic poly-alanine peptide, trehalose and doxycycline in vitro. Yet, in contrast to the above listed proteins, high molar concentrations of the ions were required, a fact that indicates that electrostatic effects are not the cause for their effects on fibril formation rates. Rather, the strongly accelerating effect of SO_4^{2-} anions and PEG appears to reflect their salting out properties. The acceleration of fibril growth rates found for trehalose and doxycycline implies that, in the animal models, these substances may not directly interfere with fibril formation but rather may retard fibril formation by inducing stress responses.

MATERIALS AND METHODS

Protein Production and Purification. Modulation of fibril formation was tested with the N-terminal domain of PABPN1 (residues 1−125 in the wild type protein). In this work, a mutant variant of the N-terminal domain with seven additional alanine residues (N-(+7)Ala) corresponding to the most extreme extension observed in human was investigated. Due to expression in pET15b, the domain is preceded by an N-terminal histidine tag which does not influence fibril formation (*22*). An exact description of this fragment, its recombinant expression and purification has been published (*22*). Bacterial expression and purification of the His-tagged deletion variant ΔN113-ΔC27 was done as previously described (*23*) with the following variations: Bacterial growth and induction was in minimal medium at 25 °C. Removal of nucleic acids and other protein contaminants was achieved by fast protein liquid chromatography using a Resource S column (GE Healthcare). Calf thymus PABPN1 was purified with minor changes as described earlier (*24*).

Peptide Synthesis. The C^{α}-peptide amide H-Ala_{17}-Lys-Tyr-Lys-NH_2 was prepared by batch solid-phase peptide synthesis using a fully automated peptide synthesizer (Applied Biosystems 431 A), standard Fmoc chemistry, HBTU/HOBt activation and NMP as the coupling solvent. Synthesis was initiated with 0.1 mmol of preloaded Tentagel S RAM-Lys-(Boc) Fmoc resin (Rapp Polymere GmbH, Germany; loading: 0.22 mmol g^{-1}) while all remaining amino acids were coupled stepwise using 10 equiv (1 mmol) of the respective Fmoc-Xaa amino acid building block. After simultaneous release from the resin by TFA treatment and side chain deprotection, the crude peptide product was precipitated with dry diethyl ether and purified by preparative RP-HPLC. The identity and purity of the synthesized peptide was checked by analytical HPLC (220 nm) and MALDI-TOF mass spectrometry (MALDI 5 V5.1.2, Kratos Kompakt) yielding satisfactory analytical data (MALDI-TOF MS, *m*/*z* calcd for $C_{72}H_{121}N_{23}O_{21}$ (1644.9): 1645.1 $[M + H]^+$). The reagents used for synthesis were products of Novabiochem, Bachem, Fluka or Merck and of highest available commercial purity.

NMR Spectroscopy and Fourier Transform Infrared Spectroscopy (FTIR). ^{1}H-spectra were recorded at a Bruker AMX 400 MHz spectrometer in 100% D_2O at 37 °C. Buffer composition was identical to that in the fibrillation assays. Infrared spectra were recorded on a Bruker IFS 66 FTIR spectrometer equipped with an MCT detector under continuous purge with dried air. A spectral resolution of 2 cm^{-1}, 256 scans, Blackman-Harris 3-Term apodization and a zero filling factor of 2 were used to collect the spectra. 20 mg/mL of fibrils of N-(+7)Ala and the respective molar mixtures with poly-alanine peptide $A_{17}KYK-NH_2$ were allowed to form in H_2O and centrifuged. The fibrils were dissolved in D_2O, centrifuged again and lyophilized twice with D_2O. Samples were prepared between two CaF_2 windows separated by a Teflon spacer of 56 μm. D_2O spectra were recorded under the same conditions and subtracted from the spectra obtained from fibrils. The final spectra were normalized to the intensity of the band at ca. 1644 cm^{-1} for better comparison.

Analysis of Fibril Formation and Preparation of Seeds. Fibrils were formed by incubating protein samples of a concentration of 1 mM in 5 mM KH_2PO_4 pH 7.5, 150 mM NaCl, 1% (w/v) NaN_3 at 37 °C. For analysis of fibril growth, ANS fluorescence was monitored as described previously (*25*). Seeds were prepared as published (*25*). Quantification of fibril formation kinetics was difficult due to the fact that fibril formation kinetics showed protein batch variations and also varied with seed preparations. For obtaining comparable data, each individual experimental setting for the comparison of fibril formation kinetics and/or lag phases was performed with identical protein and seed preparations.

Circular Dichroism (CD) Spectroscopy. CD spectra were recorded at 20 °C on a J-810 spectrapolarimeter (Jasco, Easton). The protein concentration was in the range from 0.06 mg/mL to 1.0 mg/mL as indicated in the figure legends. N-(+7)Ala was measured in 5 mM KH_2PO_4 pH 7.5, 0.15 mM NaCl in the absence or in the presence of 0.6 and 1.2 M salts with 0.1 mm quartz cuvettes over the range of 200−250 nm. The spectra shown represent the average of 10 scans run in 0.5 nm intervals, with a speed of 10 nm/min and a response of 1 s. The spectra of full-length PABPN1 from calf thymus and of the variant ΔN113-ΔC27 were measured in 20 mM Tris-Cl, pH 8.0 containing 50 mM KCl, 10% glycerol and 1 mM EDTA at 20 °C. Spectra represent an average of 20 scans recorded in 1.0 nm steps, at a scan speed of 100 nm/min and a response time of 1 s.

Miscellaneous. Quantification of soluble (monomeric) protein during and after fibril formation by reversed phase high performance liquid chromatography (RP-HPLC) has been described (*25*).

RESULTS

The N-Terminal Domain of PABPN1 Is Largely Unstructured. The analysis of poly-alanine induced fibril formation with recombinantly produced full-length PABPN1 was hampered by the contamination of fibrils with nonfibrillar aggregates. Thus, for the investigations presented here, fibrillation was studied with the N-terminal domain of PABPN1 containing seven additional alanine residues,

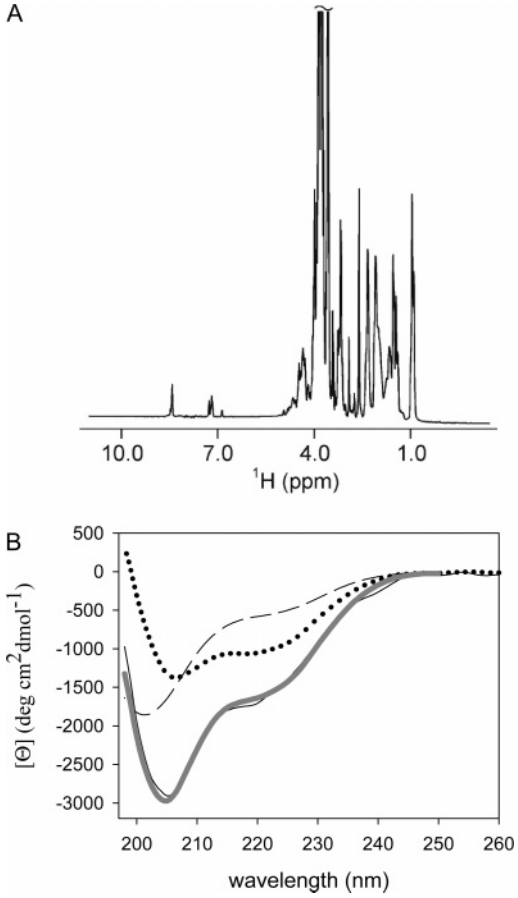

FIGURE 1: (A) ^{1}H NMR spectrum of N-(+7)Ala in D_2O at 37 °C. Missing resonance dispersion reveals a naturally unfolded polypeptide chain. Truncated signals correspond to buffer protons. (B) CD analysis of a deletion construct of PABPN1, ΔN113-ΔC27 (dotted line), N-(+7)Ala (dashed line) and the entire protein (solid line). The calculated addition spectrum = ΔN113-ΔC27 + N-(+7)Ala is indicated as a thick gray line.

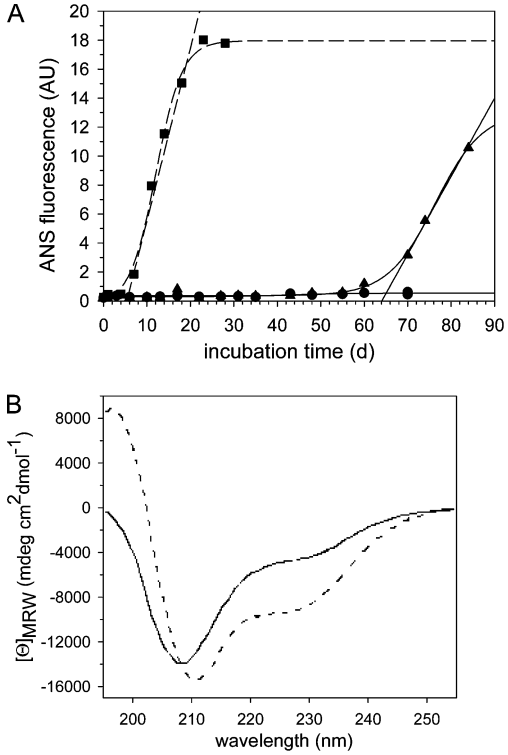

FIGURE 2: Effect of TFE on fibril formation of N-(+7)Ala. (A) Fibril formation was monitored by ANS fluorescence: control (squares); in the presence of 20% TFE (triangles); in the presence of 80% TFE (circles). ANS signals were fitted to obtain sigmoidal increases. (B) CD spectra of N-(+7)Ala in the absence (solid line) and in the presence of 80% TFE (dashed line).

N-(+7)Ala, the most extreme extension observed in humans (*3*, *22*, *25*). A previous thermodynamic analysis of N-(+7)-Ala by chemical induced unfolding had revealed a non-cooperative unfolding reaction that was interpreted as a lack of tertiary structures (data not shown). In order to confirm this assumption, structural features of N-(+7)Ala were studied by NMR spectroscopy. The ^{1}H NMR spectrum of N-(+7)Ala (Figure 1A) resembles a fully unfolded conformation because of missing resonance dispersions typically observed for chemically or thermally denatured proteins, e.g., the methyl groups around 0.7 ppm and the aromatic protons between 6 and 9 ppm show random coil chemical shifts.

CD spectroscopy was performed to investigate whether the N-terminal domain would have the same structural features in the context of full-length protein. For the analysis the deletion construct ΔN113-ΔC27, which almost complements the N-terminal domain to full-length PABPN1, was studied. The CD spectrum of ΔN113-ΔC27 was added to the spectrum of N-(+7)Ala. The calculated addition spectrum is superimposable with that of full-length PABPN1 (Figure 1B) proving that, in the detached form, the N-terminal domain possesses an identical secondary structure as in the natural context.

The Helix Stabilizer TFE Impairs Fibril Formation. Though no indication for a defined structure could be obtained by NMR, the far-UV CD spectra of N-(+7)Ala predicted the presence of more α-helical secondary elements than in the wild type fragment (*22*). We thus asked whether the α-helix inducing and stabilizing compound trifluoroethanol (TFE) would impair fibril formation (*26*). In the presence of 20% TFE, a dramatic retardation of fibril formation was observed (Figure 2A). The delay of fibril formation by ca. 40 days could be explained by evaporation of TFE caused by prolonged incubation time at 37 °C with intermittent sample removal. To analyze whether the long lag phase in the presence of TFE may be caused by an altered structure that has been induced by TFE, far-UV CD spectroscopy of the soluble fragment in the presence and absence of TFE was performed. Clearly, the presence of TFE leads to an increased amount of α-helical structures (Figure 2B). This result indicates that stabilization or induction of α-helical structure(s) suppresses fibril formation.

Stabilizing Hofmeister Anions Suppress Fibril Formation. Depending on their position in the Hofmeister series, ions either stabilize or destabilize protein structures (*27*, *28*). We reasoned that stabilization of the α-helical structure(s) as observed with TFE would impair fibril formation, consequently, high molar concentrations of the helix stabilizing salt $(NH_4)_2SO_4$ were added to N-(+7)Ala. In the following experiments, fibril formation kinetics were monitored upon seeding, since the lag phases of fibril formation usually ranged between 10 and 15 days and were often batch-dependent (for more details see Materials and Methods). Furthermore, the seeded reactions with initial linear increases of ANS fluorescence allowed a more accurate determination of elongation rates than the unseeded reactions. At both concentrations applied, 0.6 and 1.2 M, $(NH_4)_2SO_4$ accelerated

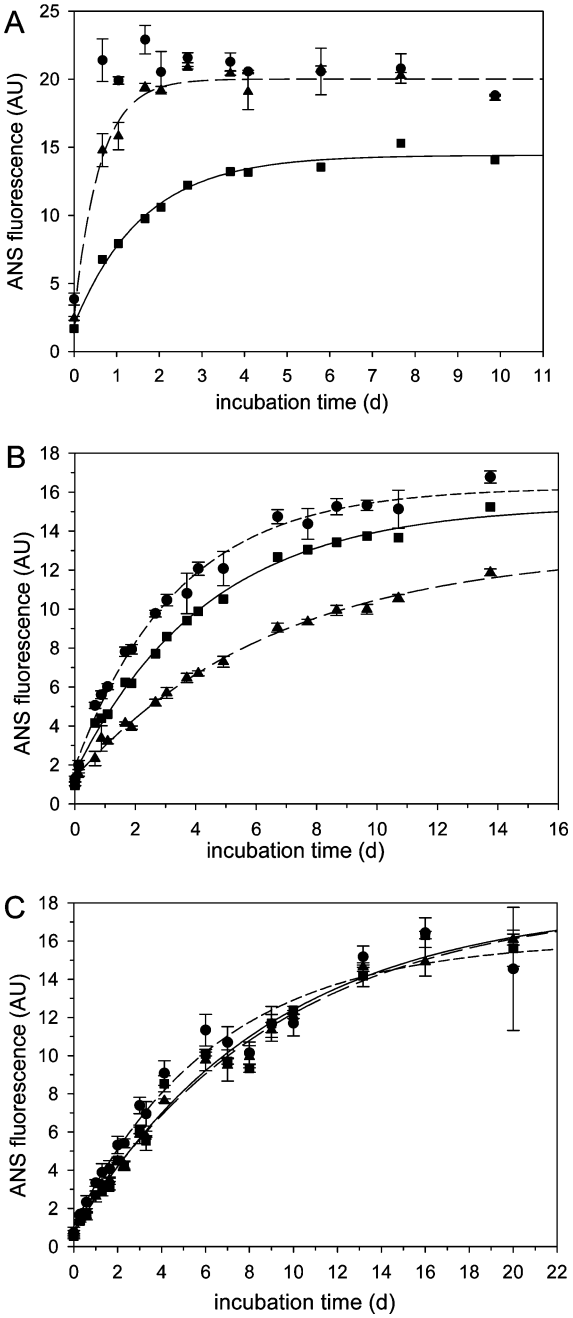

FIGURE 3: Effect of anions with NH_4^+ as the counterion on fibril formation. Fibril formation upon addition of seeds was monitored by ANS fluorescence. (A) Fibril formation in the absence (squares) and presence of 0.6 M (triangles) and 1.2 M (circles) $(NH_4)_2SO_4$. (B, C) Fibril formation in the presence of NH_4Cl (B) and NH_4NO_3 (C); symbols as in (A). The increase of ANS fluorescence was fitted to a first-order reaction to determine the initial fibril formation rates. Error bars result from three independent experiments.

fibril formation kinetics (Figure 3A, Table 1). Quantification of remaining soluble species via RP-HPLC upon completion of fibril formation revealed that the majority of the protein had been converted into fibrils (Supporting Information, Figure 1). EM analysis of the fibrils revealed that the presence of $(NH_4)_2SO_4$ influenced neither fibril lengths, widths, nor packing (data not shown). Furthermore, far-UV CD analysis showed no effect of $(NH_4)_2SO_4$ on the content of secondary structure of the soluble species (Supporting Information, Figure 2). We therefore assume that

Table 1: Fibril Formation Acceleration Factors Caused by the Addition of Salts and Arginine to the Fibrillation Reactions[a]

	SO_4^{2-}	Cl^-	NO_3^-
NH_4^+			
0.6 M	3.8	0.6	0.9
1.2 M	(>30)	1.3	1.2
Na^+			
0.6 M	(>200)	1.1	1.3
1.2 M	(>300)	2.7	2.3
arginine			
0.6 M	0.3	0.4	
1.2 M	1.8	0.5	

[a] Increases of ANS fluorescence were fitted to first-order reactions to determine the initial fibril formation rates. The increases of ANS fluorescence in the absence of salts were defined as 1.

$(NH_4)_2SO_4$ affects the fibril formation reaction itself, e.g., stabilization of fibrillation intermediates or the fibrils themselves.

Numerous investigations demonstrate that in particular anions facilitate fibril formation: An acceleration of fibril formation by millimolar concentrations of sulfate anions was observed with α-synuclein, β_2-microglobulin and glucagon (*18*, *19*, *21*). These results were interpreted by electrostatic effects of the anions on prefibrillar species. In order to explore whether the sulfate anion or the ammonium cation of $(NH_4)_2SO_4$ causes the observed acceleration of fibrillation rates, Cl^- and NO_3^- with NH_4^+ as the counterion were tested for their effects. With NH_4Cl, an acceleration of fibril formation by a factor of 1.3 was observed at a concentration of 1.2 M, while in the presence of 0.6 M NH_4Cl, a retardation of fibril formation was found (Figure 3B). A possible influence of NH_4Cl on the secondary structure content of the soluble species was excluded by far-UV CD spectroscopy (data not shown). With NH_4NO_3, even at the high molar concentration of 1.2 M, no significant influence on the kinetics of fibril formation was detected (Figure 3C). Thus, the acceleration of fibril formation observed in the presence of $(NH_4)_2SO_4$ should be mediated by the anion of the salt. Furthermore, since the ionic strengths of $(NH_4)_2SO_4$, NH_4Cl, and NH_4NO_3 differ only by a factor of 2, the effects observed here are due to the specific anion and not different ionic strengths.

The anions tested so far were added together with Na^+ as the counterion in order to detect effects of cations on fibrillation kinetics. Na_2SO_4 led to a comparable enhancement of fibril formation rates as $(NH_4)_2SO_4$ (Figure 4A). NaCl, at 1.2 M, accelerated fibril formation by a factor of 2.6, while at 0.6 M the effect of NaCl was marginal (Figure 4B, Table 1). The fact that 1.2 M NH_4Cl gave rise to a 1.3-fold acceleration of fibril formation (Figure 3B) indicates that to a certain extent also cations influence the fibril formation process. Surprisingly, Na^+ had a slightly more accelerating effect than the more kosmotropic NH_4^+ cation (*28*). Again no influence of the ions on the structure of the soluble species could be detected by CD analysis (data not shown). As with the other salts, only the rate of fibril formation was influenced and not the final amount of fibrillar species (Supporting Information, Figure 1). In a similar way as NaCl, $NaNO_3$ accelerated fibril formation (Figure 4C).

In summary, the most prominent effects were obtained with SO_4^{2-} anions (Table 1). This result confirms those of others who showed that sulfate anions can play a major role during in vitro fibril formation processes (*18*, *19*, *21*). Since

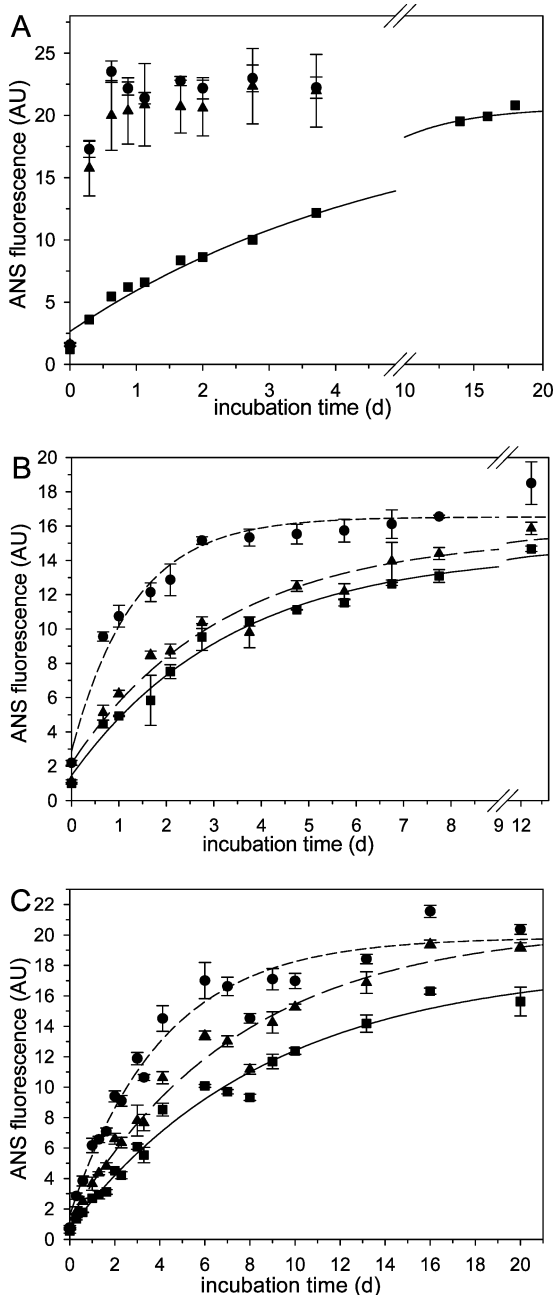

FIGURE 4: Effect of anions on fibril formation with Na^+ as the counterion. Fibril formation was monitored as indicated in the legend to Figure 3. (A) Fibril formation in the absence (squares) and presence of 0.6 M (triangles) and 1.2 M (circles) Na_2SO_4. (B, C) Effect of NaCl (B) and of $NaNO_3$ (C) on fibril formation; symbols as in (A).

an influence of the salts on the secondary structural content of the monomeric species was excluded via CD spectroscopy, we conclude that the salts influence potential conformational intermediates on the way to the fibrillar state or ease the association of soluble species with already existing fibrillar species.

The Effect of L*-Arginine on Fibril Formation Depends Primarily on the Counterion.* Protein aggregation can also be suppressed by the amino acid L-arginine which is used in industry for in vitro refolding of denatured proteins. The solubilizing effect of L-arginine on aggregation-prone folding intermediates often increases renaturation yields (*29*, *30*). Thus, we tested the influence of L-arginine on fibril formation kinetics at the high molar concentrations (0.6 and 1.2 M)

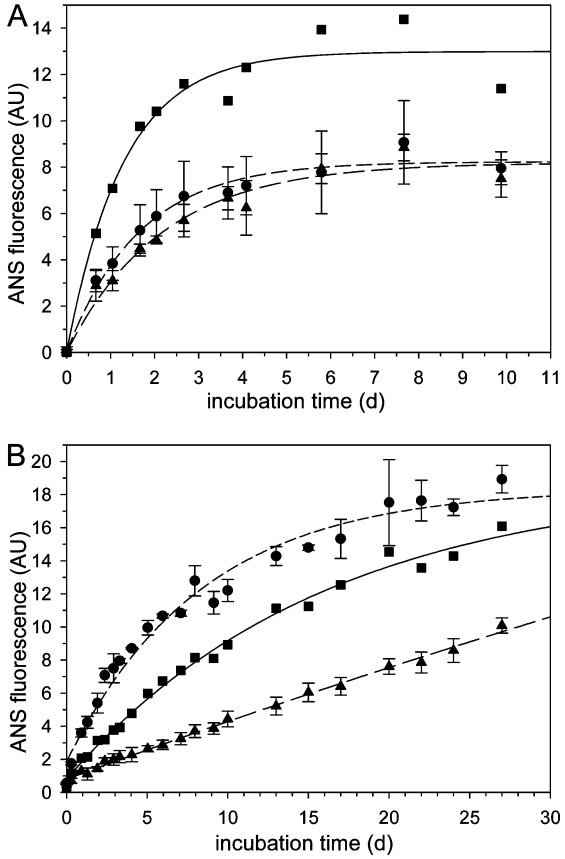

FIGURE 5: Effect of L-arginine on fibril formation rates. (A) Fibril formation in the absence (squares) and presence of 0.6 M (triangles) and 1.2 M (circles) arginine/Cl. (B) Effect of arginine/SO_4 on fibril formation. Symbols as in (A). The increase of ANS fluorescence was fitted to a first-order reaction to determine the initial fibril formation rates. Error bars result from three independent experiments.

that are typical in industrial in vitro renaturation processes. To assess counterion effects, L-arginine titrated with either HCl or H_2SO_4 was used. L-Arginine/Cl retarded fibril formation (Figure 5A). Quantification of residual monomeric species after completion of fibril formation revealed a significant amount of non-fibrillized soluble protein (Supporting Information, Figure 1). When arginine/SO_4 was present, a retardation of fibril formation was only observed at 0.6 M arginine/SO_4, while at 1.2 M, kinetics were accelerated by a factor of ca. 2 (Figure 5B). Here, quantification of soluble species after completion of fibril formation showed comparable levels of soluble species of the control sample without arginine/SO_4 and that containing 1.2 M arginine/SO_4 (Supporting Information, Figure 1). Quantification of nonfibrillized protein could not be performed with the sample containing 0.6 M aginine/SO_4, since even after 30 days, ANS fluorescence signals had not reached a plateau (Figure 5B). Since, with arginine/Cl, fibril formation rates were reduced whereas, with 1.2 M arginine/SO_4, fibrillation was accelerated, we conclude that also here the SO_4^{2-} anion is responsible for the enhanced fibril elongation rates.

Poly-ethylene Glycol Accelerates Fibril Formation. Another stabilizing agent is poly-ethylene glycol which is used in crystallography due to its stabilizing properties (*31*). The poly-alcohol has also been tested as an artificial crowding agent during fibrillation of α-synuclein (*32*). Here, PEG-8000 with a similar molecular mass as N-(+7)Ala was tested. At both a 5- and 10-fold molar excess, PEG accelerated fibril

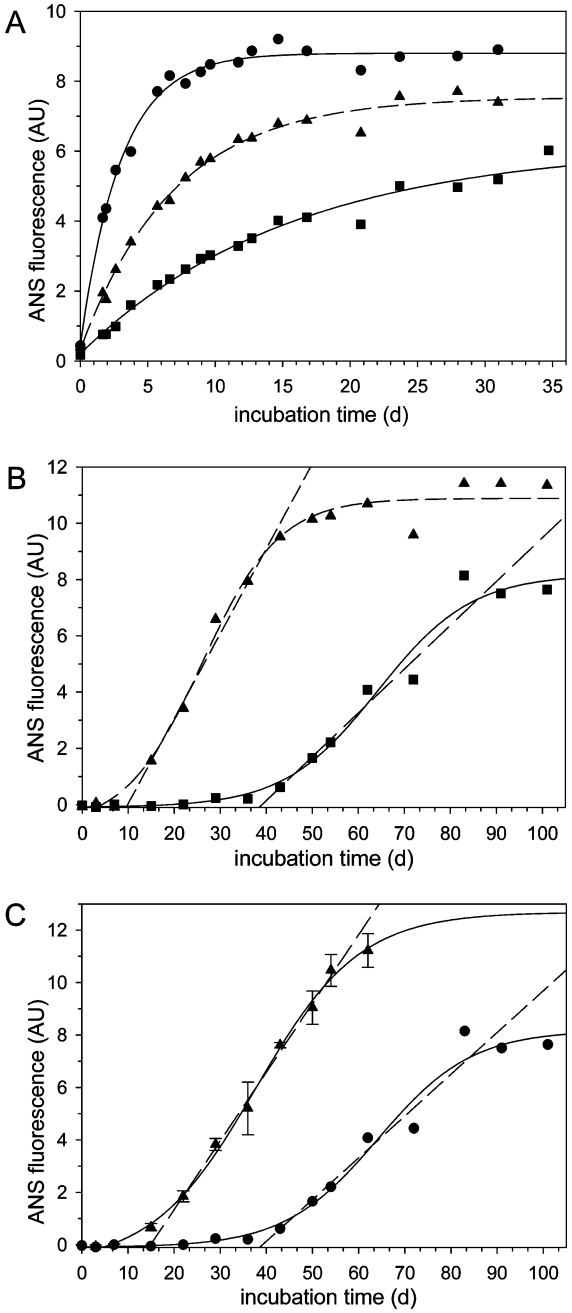

FIGURE 6: Influence of the crowding agent PEG and the low molecular weight substances trehalose and doxycycline on fibril formation of N-(+7)Ala. (A) 1 mM N-(+7)Ala was incubated in the absence (squares) and in the presence of 5 mM (triangles) and 10 mM (circles) PEG 8000. Fibril formation upon addition of seeds was monitored by ANS fluorescence. The increase of ANS fluorescence in the presence of seeds was fitted to a first-order reaction to determine the initial fibril formation rates. (B) Unseeded fibril formation in the absence (squares) and presence of 250 mM trehalose (triangles). (C) Unseeded fibril formation of 1 mM N-(+7)Ala in the absence (circles) and presence of 1 mM doxycycline (triangles). ANS signals were fitted to obtain sigmoidal increases. In (B) and (C), the slopes of ANS increases in the linear range are indicated by interrupted lines. Error bars result from three independent experiments.

formation kinetics (Figure 6A), confirming our assumption that salting out effects play a crucial role during fibrillation of N-(+7)Ala.

The Potential Therapeutic Agents Trehalose and Doxycycline Accelerate Fibril Formation. Similarly to L-arginine, the disaccharide trehalose has been reported to reduce both in vitro and in vivo stress induced protein misfolding (*33*−*35*). For in vitro stabilization of a model protein, trehalose concentrations up to 0.8 M have been demonstrated to increase thermodynamic stability (*33*). In vivo, trehalose has been shown to display beneficial effects in animal models for Huntington's disease and OPMD (*16*, *36*). Therefore, a potential effect of trehalose on the fibrillation of N-(+7)Ala was tested. Unexpectedly, the presence of 250 mM trehalose resulted in a reduction of the lag phase and an acceleration of fibrillation kinetics (Figure 6B; Supporting Information, Table 1).

As a second compound that has been described to attenuate and delay OPMD symptoms in a mouse model (*15*), doxycycline was added in an equimolar concentration to unseeded fibrillation samples. As trehalose, doxycycline accelerated fibril formation (Figure 6C; Supporting Information, Table 1). This finding indicates that even though tetracycline derivatives have been shown to interfere with fibril formation of Aβ 1−42 peptide and transthyretin in vitro (*37*, *38*), reduction of fibril formation or even resolution of fibrils by tetracycline derivatives may not be a general feature of these compounds.

A Synthetic Poly-alanine Peptide Stimulates Fibril Formation and Is Integrated into N-(+7)Ala Fibrils. Poly-alanine peptides have been described to exhibit a high propensity to undergo in vitro fibril formation (*39*, *40*). Thus, we asked whether a poly-alanine peptide containing 17 alanines as present in N-(+7)Ala would accelerate fibril formation. A "pure" poly-alanine peptide could not be synthesized due to its extremely poor solubility. Thus, the influence on fibril formation of N-(+7)Ala was tested with the peptide A_{17}-KYK-NH_2, that possessed additional solubilizing C-terminal residues. Addition of 0.1 mM A_{17}KYK-NH_2 to samples containing soluble 1 mM N-(+7)Ala reduced the lag phase of fibril formation and enhanced fibril growth rates (Figure 7A; Supporting Information, Table 1). The decrease of both soluble N-(+7)Ala and peptide species after an incubation time of 15 days, as quantified by RP-HPLC, indicated the conversion of soluble into fibrillar species (Figure 7B). The ability of the peptide to undergo a conformational change from α-helical to β-secondary structure was confirmed by CD analysis (Supporting Information, Figure 3). Removal of the loosely with the fibrils associated peptide by washing and subsequent solubilization of the fibrils with guanidinium thiocyanate allowed quantification of the peptide fraction which had been integrated into the fibrils (Supporting Information, Figure 4). Furthermore, the sample containing peptide alone did not give rise to increased ANS fluorescence within 15 days, in contrast to the reaction in which both peptide and N-(+7)Ala had been present (Figure 7A). This observation suggests that rises in ANS signals result from peptide and N-(+7)Ala in mixed fibrils. Visualization of the fibrils by EM revealed no differences to those fibrils that we obtain in the absence of peptide (Figure 7C).

The influence of A_{17}KYK-NH_2 on the secondary structure elements of fibrils was investigated by FTIR spectroscopy (Figure 7D). The shape of the amide I band of the N-(+7)-Ala fibrils revealed bands at 1624 cm^{-1} and 1695 cm^{-1} which clearly indicate the formation of antiparallel β-sheets (*41*−*43*). The broad shoulder at ca. 1644 cm^{-1} may be assigned to unordered structures. All spectra have been normalized

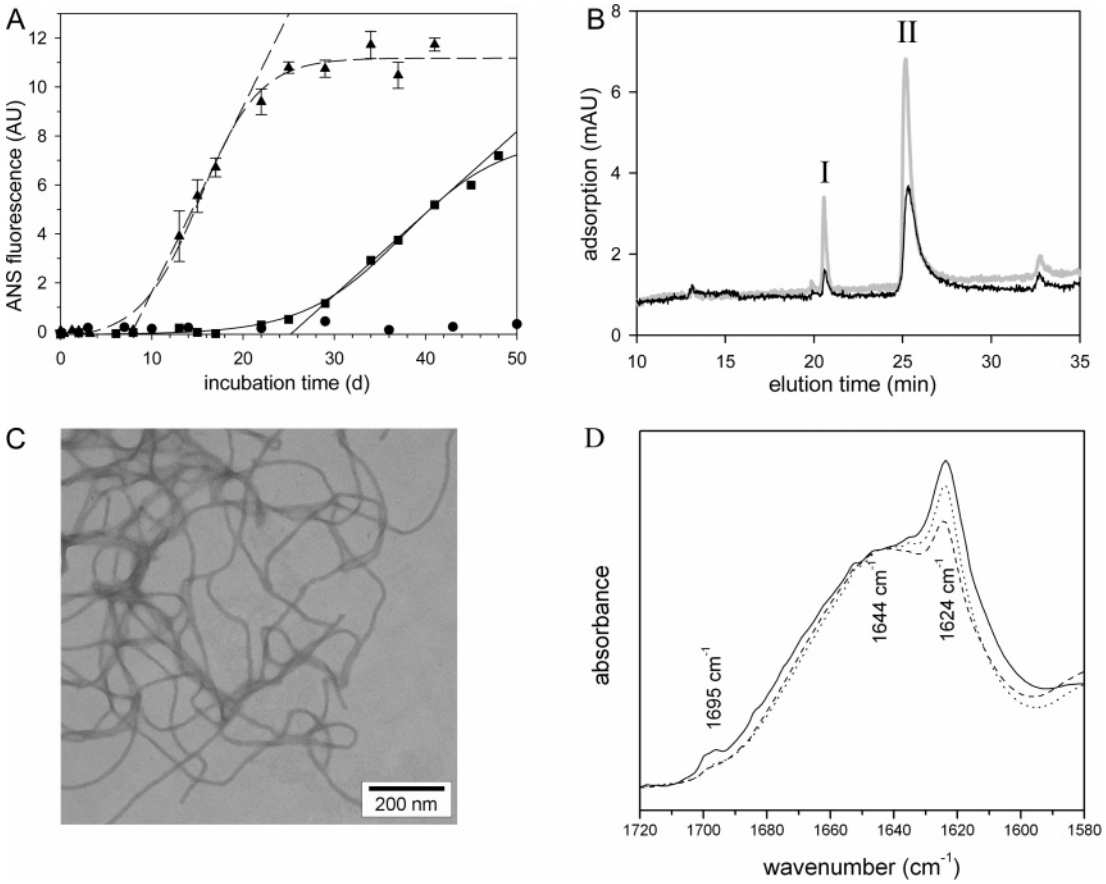

FIGURE 7: Influence of the poly-alanine peptide $A_{17}KYK\text{-}NH_2$ on fibril formation of N-(+7)Ala. (A) Unseeded fibril formation of 1 mM N-(+7)Ala in the absence (squares) and presence of 0.1 mM $A_{17}KYK\text{-}NH_2$ (triangles). For control, ANS fluorescence with 0.1 mM $A_{17}KYK\text{-}NH_2$ in the absence of N-(+7)Ala was tested (circles). The slopes of ANS increases in the linear range are indicated by interrupted lines. (B) RP-HPLC chromatograms of samples from the fibrillation reaction containing N-(+7)Ala and $A_{17}KYK-NH_2$, before incubation (gray line) and after 15 days (black). Peak I corresponds to soluble $A_{17}KYK\text{-}NH_2$ and peak II to soluble N-(+7)Ala. (C) Electron micrograph of putative "mixed" fibrils consisting of N-(+7)Ala and $A_{17}KYK\text{-}NH_2$. (D) Normalized FTIR spectra of N-(+7)Ala fibrils in the absence (solid line) and presence of poly-alanine peptide $A_{17}KYK\text{-}NH_2$. 1 mM N-(+7)Ala was incubated for 15 days with 0.1 mM (dashed line) and 0.4 mM (dotted line) $A_{17}KYK\text{-}NH_2$. Spectra were measured in D_2O at 20 °C and normalized to the intensity of the band at ca. 1644 cm^{-1}.

to the band at 1644 cm^{-1} to directly visualize the changes in the β-sheet content of the protein peptide fibrils. With increasing amounts of the peptide $A_{17}KYK\text{-}NH_2$ from 0.1 to 0.4 mM in the protein peptide mixture, the intensity of the band at 1624 cm^{-1} increased, indicating an increased amount of β-sheets in the fibrils.

DISCUSSION

The result that fibril formation rates are enhanced by anions was not unexpected since several publications have demonstrated a stimulating effect of anions on fibril formation (*18*, *19*, *21*). It has been speculated that, during fibrillation of α-synuclein, β_2-microglobulin and glucagon, the anions act via their ionic interactions, and their influence on fibril formation corresponds to the electroselectivity series, i.e., the potency of anions to bind to anion exchange material (*18*, *19*, *21*). However, in these reports salt effects were already observed in the millimolar range. In contrast, here, the anions only exerted effects at high molar concentrations where Hofmeister ions display their activities. In the case of α-synuclein, the effect of anions on fibril formation was interpreted by an anion-induced structure formation of the otherwise natively unfolded protein (*19*). Likewise, under acidic conditions, Na_2SO_4 has been shown to lead to structural changes in β_2-microglobulin and thus an acceleration of fibril formation (*18*). More generally, a prominent role of physiological anions and poly-anions in the fibrillation process is being assumed (*44*, *45*).

Salt-elicited structural changes in N-(+7)Ala were not observed by CD spectroscopy though small amounts of structurally divergent species that could serve as fibrillation intermediates may not be detected via this technique. On the other hand, not even fibril morphology was influenced by the salts. Fibrils formed in the presence of the tested anions never differed in their length, width or packing from those formed in the absence of salts. Thus, sulfate ion induced changes on the level of fibril morphology and packing as have been reported for Abeta peptides (*46*) do not occur under the conditions investigated here. Taken together, our data allow the conclusion that anions influence fibrillation of N-(+7)Ala probably only via their salting out properties. This assumption is confirmed by the effect of PEG, an uncharged substance that acts as a molecular crowding agent and protein stabilizer based on its—without being a salt—"salting out" properties. The significantly smaller effects of cations compared to anions is noteworthy and supports our assumption that electrostatic effects may be of subordinate importance. As the isoelectric point of

N-(+7)Ala is at 4.6, cations should enhance fibrillation at neutral pH via reduction of charge repulsion.

Both trehalose and doxycycline, at the concentrations tested here, reduced the lag phase of fibril formation, a result which is not compatible with the beneficial effects of these substances in the OPMD animal models (*15*, *16*). Of course it is not clear which intracellular concentrations of trehalose and doxycycline were present and effective in vivo. Furthermore, both compounds could elicit a series of intracellular responses like increased chaperone expression and/or enhanced proteolytic breakdown. While the in vivo effects of trehalose and doxycycline in OPMD models require comprehensive cell-biological testing, the data presented here provide strong evidence that both substances might interact with either soluble or prefibrillar intermediates in such a way that fibril formation is accelerated.

Though at odds with its in vivo effect in OPMD models, the reduction of the lag phase by the osmolyte trehalose can be explained on a biophysical level: An osmolyte-induced contraction of unfolded proteins due to unfavorable interactions with the polypeptide backbone—which is more exposed in the unfolded state—has been documented (*47*, *48*). The contraction to a more folded conformation by trehalose in the case of the N-terminal domain of PABPN1 would be the fibrillar and not the soluble state. If that should hold true, the effect of trehalose on fibril formation could mechanistically resemble that of stabilizing Hofmeister salts. In the full-length protein, however, trehalose or—more generally—osmolytes could lead to an increased interaction of the N-terminal domain with more compactly folded segments of PABPN1 and, via this way, the compounds may reduce OPMD symptoms.

In an experimental setting related to peptide A_{17}KYK-NH_2-induced fibrillation of N-(+7)Ala presented here, Lindquist and co-workers demonstrated fibril formation of the full-length NM domain from Sup35 induced by single peptides derived from Sup35 (*49*). The observation that peptide A_{17}KYK-NH_2 stimulated fibril formation of N-(+7)-Ala shows that a poly-alanine stretch of 17 alanines is sufficient for amyloidogenicity. The existence of mixed fibrils with both N-(+7)Ala and the peptide being present in the same fibril is very likely, since only solubilization of the fibrils with guanidinium thiocyanate led to the recovery of both the peptide and N-(+7)Ala. Furthermore, FTIR spectroscopy showed that the amount of β-sheets depended on the concentration of A_{17}KYK-NH_2 in the fibrillation samples. Via EM analysis no differences of the fibrils formed in the presence or absence of A_{17}KYK-NH_2 were detected. It is noteworthy that, throughout our analyses via EM, fibrils always displayed diameters of 5−7 nm, which is in the range of diameters of fibrils formed from short poly-alanine peptides of 11, 13 and 20 residues (*39*).

Taking into account that several recent reports clearly demonstrate fibril subtypes depending on the conditions under which they form (*50*−*53*), future analyses have to clarify whether the fibrils formed in the presence of salts and low molecular weight additives possess the same properties as those formed in the absence of additives.

ACKNOWLEDGMENT

We thank Gerd Hause for confirming the existence of fibrils by EM. We are grateful to Rainer Rudolph and Marcus Fändrich for critical comments on the manuscript.

SUPPORTING INFORMATION AVAILABLE

Quantification by RP-HPLC of soluble species after fibrillation, the CD analysis of N-(+7)Ala in the absence and presence of $(NH_4)_2SO_4$, CD spectra of the peptide A_{17}-KYK-NH_2 before and after incubation at room temperature, and a table summarizing the effect of a peptide and low molecular weight compounds on fibril elongation rates. This material is available free of charge via the Internet at http://pubs.acs.org.

REFERENCES

1. Wahle, E. (1991) A novel poly(A)-binding protein acts as a specificity factor in the second phase of messenger RNA polyadenylation, *Cell 66*, 759−768.
2. Wahle, E., and Rüegsegger, U. (1999) 3′-End processing of premRNA in eukaryotes, *FEMS Microbiol. Rev. 23*, 277−295.
3. Brais, B., Bouchard, J.-P., Xie, Y.-G., Rochefort, D. L., Chrétien, N., Tomé, F. M. S., Lafrenière, R. G., Rommens, J. M., Uyama, E., Nohira, O., Blumen, S., Korcyn, A. D., Heutink, P., Mathieu, J., Duranceau, A., Codère, F., Fardeau, M., and Rouleau, G. A. (1998) Short GCG expansions in the *PABP2* gene cause oculopharyngeal muscular dystrophy, *Nat. Genet. 18*, 164−167.
4. Tomé, F. M. S., Askanas, V., Engel, W. K., Alvarez, R. B., and Lee, C. S. (1989) Nuclear inclusions in innervated cultured muscle fibers from patients with oculopharyngeal muscular dystrophy, *Neurology 39*, 926−932.
5. Tomé, F. M. S., Chateau, D., Helbling-Leclerc, A., and Fardeau, M. (1997) Morphological changes in muscle fibers in oculopharyngeal muscular dystrophy, *Neuromuscular Disord. 7*, S63−S69.
6. Calado, A., Tomé, F. M. S., Brais, B., Rouleau, G. A., Kühn, U., Wahle, E., and Carmo-Fonseca, M. (2000) Nuclear inclusions in oculopharyngeal muscular dystrophy consist of poly(A) binding protein 2 aggregates which sequester poly(A) RNA, *Hum. Mol. Genet. 9*, 2321−2328.
7. Uyama, E., Tsukahara, T., Goto, K., Kurano, Y., Ogawa, M., Kim, Y.-J., Uchino, M., and Arahata, K. (2000) Nuclear accumulation of expanded *PABP2* gene product in oculopharyngeal muscular dystrophy, *Muscle Nerve 23*, 1549−1554.
8. Abu-Baker, A., and Rouleau, G. A. (2006) Oculopharyngeal muscular dystrophy: Recent advances in the understanding of the molecular pathogenic mechanisms and treatment strategies, *Biochim. Biophys. Acta 1772*, 173−185.
9. Fan, X., Dion, P., Laganiere, J., Brais, B., and Rouleau, G. A. (2001) Oligomerization of polyalanine expanded PABPN1 facilitates nuclear protein aggregation that is associated with cell death, *Hum. Mol. Genet. 10*, 2341−2351.
10. Chartier, A., Benoit, B., and Simonelig, M. (2006) A *Drosophila* model of oculopharyngeal muscular dystrophy reveals intrinsic toxicity of PABPN1, *EMBO J. 25*, 2253−2262.
11. Abu-Baker, A., Messaed, C., Laganiere, J., Gaspar, C., Brais, B., and Rouleau, G. A. (2003) Involvement of the ubiquitin-proteasome pathway and molecular chaperones in oculopharyngeal muscular dystrophy, *Hum. Mol. Genet. 12*, 2609−2623.
12. Bao, Y. P., Cook, L. J., O'Donovan, D., Uyama, E., and Rubinsztein, D. C. (2002) Mammalian, yeast, bacterial, and chemical chaperones reduce aggregate formation and death in a cell model of oculopharyngeal muscular dystrophy, *J. Biol. Chem. 277*, 12263−12269.
13. Bao, Y. P., Sarkar, S., Uyama, F., and Rubinsztein, D. C. (2004) Congo red, doxycycline, and HSP70 overexpression reduce aggregate formation and cell death in cell models of oculopharyngeal muscular dystrophy, *J. Med. Genet. 41*, 47−51.
14. Wang, Q., Mosser, D. D., and Bag, J. (2005) Induction of Hsp70 expression and recruitment of Hsc70 and Hsp70 in the nucleus reduce aggregation of a polyalanine expansion mutant of PABPN1 in HeLa cells, *Hum. Mol. Genet. 14*, 3673−3684.
15. Davies, J. E., Wang, L., Garcia-Oroz, L., Cook, L. J., Vacher, C., O'Donovan, D. G., and Rubinsztein, D. C. (2005) Doxycycline

attenuates and delays toxicity of the oculopharyngeal mutation in transgenic mice, *Nat. Med. 11*, 672−677.
16. Davies, J. E., Sarkar, S., and Rubinsztein, D. C. (2006) Trehalose reduces aggregate formation and delays pathology in a transgenic mouse model of oculopharyngeal muscular dystrophy, *Hum. Mol. Genet. 15*, 23−31.
17. Nielsen, L., Khurana, R., Coats, A., Frokjaer, S., Brange, J., Vyas, S., Uversky, V. N., and Fink, A. L. (2001) Effect of environmental factors on the kinetics of insulin fibril formation: elucidation of the molecular mechanism, *Biochemistry 40*, 6036−6046.
18. Raman, B., Chatani, E., Kihara, M., Ban, T., Sakai, M., Hasegawa, K., Naiki, H., Rao, Ch. M., and Goto, Y. (2005) Critical balance of electrostatic and hydrophobic interactions is required for β_2-microglobulin amyloid fibril growth and stability, *Biochemistry 44*, 1288−1299.
19. Munishkina, L. A., Henriques, J., Uversky, V. N., and Fink, A. L. (2004) Role of protein−water interactions and electrostatics in α-synuclein fibril formation, *Biochemistry 43*, 3289−3300.
20. Pedersen, J. S., Christensen, G., and Otzen, D. E. (2004) Modulation of S6 fibrillation by unfolding rates and gatekeeper residues, *J. Mol. Biol. 341*, 575−588.
21. Pedersen, J. S., Flink, J. M., Dikov, D., and Otzen, D. E. (2006) Sulfates dramatically stabilize a salt-dependent type of glucagons fibrils, *Biophys. J. 90*, 4181−4194.
22. Scheuermann, T., Schulz, B., Blume, A., Wahle, E., Rudolph, R., and Schwarz, E. (2003) Trinucleotide expansions leading to an extended poly-L-alanine segment in the poly (A) binding protein PABPN1 cause fibril formation, *Protein Sci. 12*, 2685−2692.
23. Kühn, U., Nemeth, A., Meyer, S., and Wahle, E. (2003) The RNA binding domains of the nuclear poly(A) binding protein, *J. Biol. Chem. 278*, 16916−16925.
24. Wahle, E., Lusig, A., Jenö, P., and Maurer, P. (1993) Mammalian poly(A)-binding protein II. Physical properties and binding to polynucleotides, *J. Biol. Chem. 268*, 2937−2945.
25. Lodderstedt, G., Hess, S., Hause, G., Scheuermann, T., Scheibel, T., and Schwarz, E. (2007) Effect of oculopharyngeal muscular dystrophy-associated extension of seven alanines on the fibrillation properties of the N-terminal domain of PABPN1, *FEBS J. 274*, 346−355.
26. Luo, P., and Baldwin, R. L. (1997) Mechanism of helix induction by trifluoroethanol: a framework for extrapolating the helix-forming properties of peptides from trifluoroethanol/water mixtures back to water, *Biochemistry 36*, 8413−8421.
27. Baldwin, R. L. (1996) How Hofmeister ion interactions affect protein stability, *Biophys. J. 71*, 2056−2063.
28. Hofmeister, F. (1888) On the understanding of the effects of salts. On regularities in the precipitating effects of salts and their relationship to their physiological behaviour, *Arch. Exp. Pathol. Pharmakol. (Leipzig) 24*, 247−260.
29. De Bernadez Clark, E., Schwarz, E., and Rudolph, R. (1999) Inhibition of aggregation side reactions during in vitro protein folding, in *Amyloid, Prions, and other Protein Aggregates*, *Methods Enzymol.* (Wetzel, R., Ed.) Vol. 309, pp 217−236, Academic Press, San Diego.
30. Reddy, R. C. K., Lilie, H., Rudolph, R., and Lange, C. (2005) L-Arginine increases the solubility of unfolded species of hen egg white lysozyme, *Protein Sci. 14*, 929−935.
31. Shulgin, I. L., and Ruckenstein, E. (2006) Preferential hydration and solubility of proteins in aqueous solutions of polyethylene glycol, *Biophys. Chem. 120*, 188−198.
32. Muniskina, L. A., Cooper, E. M., Uversky, V. N., and Fink, L. A. (2004) The effect of macromolecular crowding on protein aggregation and amyloid fibril formation, *J. Mol. Recognit. 17*, 456−464.
33. Chen, L., Cabrita, G. J., Otzen, D. E., and Melo, E. P. (2005) Stabilization of the ribosomal protein S6 by trehalose is counter-balanced by the formation of a putative off-pathway species, *J. Mol. Biol. 351*, 402−416.
34. Singer, M. A., and Lindquist, S. (1998) Multiple effects of trehalose on protein folding *in vitro* and *in vivo*, *Mol. Cell. 1*, 639−648.
35. Arora, A., Ha, C., and Park, C. B. (2004) Inhibition of insulin amyloid formation by small stress molecules, *FEBS Lett. 564*, 121−125.
36. Tanaka, M., Machida, Y., Niu, S., Ikeda, T., Jana, N. R., Doi, H., Kurosawa, M., Nekooki, M., and Nukina, N. (2004) Trehalose alleviates polyglutamine-mediated pathology in a mouse model of Huntington disease, *Nat. Med. 10*, 148−154.
37. Forloni, G., Colombo, L., Girola, L., Tagliavini, F., and Salmona, M. (2001) Anti-amyloidogenic activity of tetracyclines: studies in vitro, *FEBS Lett. 487*, 404−407.
38. Cardoso, I., Merlini, G., and Saraiva, M. J. (2003) 4′-Iodo-4′-deoxydoxorubicin and tetracyclines disrupt transthyretin amyloid fibrils in vitro producing noncytotoxic species: screening for TTR fibril disrupters, *FASEB J. 17*, 803−809.
39. Shinchuk, L. M., Sharma, D., Blondelle, S. E., Reixach, N., Inouye, H., and Kirschner. D. A. (2005) Poly-(L-alanine) expansions form core β-sheets that nucleate amyloid assembly, *Proteins 61*, 579−589.
40. Krimm, S., and Bandekar, J. (1986) Vibrational spectroscopy and conformation of peptides, polypeptides, and proteins, *Adv. Protein. Chem. 38*, 181−364.
41. Jackson, M., and Mantsch, H. H. (1991) Protein secondary structure from FT-IR spectroscopy: Correlation with dihedral angles from three-dimensional Ramachandran plots, *Can. J. Chem. 69*, 1639−1642.
42. Zandomeneghi, G., Krebs, M. R. H., McCammon, M. G., and Fändrich, M. (2004) FTIR reveals structural differences between native β-sheet proteins and amyloid fibrils, *Protein Sci. 13*, 3314−3321.
43. Blondelle, S. E., Forood, B., Houghten, R. A., and Pérez-Paya, E. (1997) Polyalanine-based peptides as models for self-associated β-pleated-sheet complexes, *Biochemistry 36*, 8393−8400.
44. Calami, M., Kumita, J. R., Mifsud, J., Parrini, C., Ramazzotti, M., Ramponi, G., Taddei, N., Chiti, F., and Dobson, C. M. (2006) Nature and significance of the interaction between amyloid fibrils and biological polylectrolytes, *Biochemistry 45*, 12806−12815.
45. Kisilevsky, R. (2000) Amyloidogenesis—unquestioned answers and unanswered questions, *J. Struct. Biol. 130*, 99−108.
46. Fraser, P. E., Nguyen, J. T., Chin, D. T., and Kirschner, D. A. (1992) Effects of sulfate ions on Alzheimer β/A4 peptide assemblies: Implications for amyloid fibril-proteoglacan interactions, *J. Neurochem. 59*, 1531−1540.
47. Xie, G., and Timasheff, S. N. (1997) The thermodynamic mechanism of protein stabilization by trehalose, *Biophys. Chem. 64*, 25−43.
48. Qu, Y., Bolen, C. L., and Bolen, D. W. (1998) Osmolyte-driven contraction of a random coil protein, *Proc. Natl. Acad. Sci. U.S.A. 95*, 9268−9273.
49. Tessier, P. M., and Lindquist, S. (2007) Prion recognition elements govern nucleation, strain specificity and species barriers, *Nature 447*, 556−561.
50. Gast, K., Modler, A. J., Damaschun, H., Kröber, R., Lutsch, G., Zirwer, D., Golbik, R., and Damaschun, G. (2003) Effect of environmental conditions on aggregation and fibril formation of barstar, *Eur. Biophys. J. 32*, 710−723.
51. Pedersen, J. S., Dikov, D., Flink, J. L., Hjuler, H. A., Christiansen, G., and Otzen, D. E. (2006) The changing face of glucagons fibrillation: structural polymorphism and conformational imprinting, *J. Mol. Biol. 355*, 501−523.
52. Petkova, A. T., Leapman, R. D., Guo, Z., Yau, W.-M., Mattson, M. P., and Tycko, R. (2005) Self-propagating, molecular-level polymorphism in Alzheimer's β-amyloid fibrils, *Science 307*, 262−265.
53. Tanaka, M., Chien, P., Naber, N., Cooke, R., and Weissman, J. S. (2004) Conformational variations in an infectious protein determine prion strain differences, *Nature 428*, 323−327.

BI701322G